https://doi.org/10.5194/amt-2019-300
Preprint. Discussion started: 2 October 2019

Atmospheric Measurement Techniques Discussions

Aerosol optical characteristics in the urban area of Rome, Italy, and their impact on the UV index.

Monica Campanelli[1], Anna Maria Siani[2], Alcide di Sarra[3], Anna Maria Iannarelli[4], Paolo Sanò[1], Henri Diémoz[5], Giampietro. Casasanta[1], Marco Cacciani[2], Luca Tofful[6], Stefano Dietrich[2]

[1] Institute of Atmospheric Sciences and Climate, National Research Council, Rome, Italy
[2] Sapienza University of Rome, Department of Physics, Rome, Italy
[3] Dipartimento Ambiente, Cambiamenti Globali e Sviluppo Sostenibile, Ente per le Nuove Tecnologie, l'Energia e l'Ambiente, Rome, Italy
[4] SERCO, Italy
[5] Agenzia Regionale Protezione Ambientale-Valle d'Aosta, ARPA-VDA, Italy
[6] Institute of Atmospheric pollution, National Research Council, Italy

Abstract

The aerosol optical characteristics in the urban area of Rome were retrieved over a period of 7 years from March to September 2010-2016. The impact of aerosol single scattering albedo (SSA), optical depth (AOD), estimated at 400 nm, and Ångström exponent on the ultraviolet (UV) index has been analyzed. Aerosol optical properties are provided by a PREDE-POM sun-sky radiometer of the ESR/SKYNET network and the UV index values were retrieved by a Brewer spectrophotometer both located in Rome. Chemical characterization of urban PM10 (particulate matter 10 micrometers or less in diameter) samples, collected during the URBan Sustainability Related to Observed and Monitored Aerosol (URBS ROMA) intensive filed campaign held in summer 2011 in the same site, was performed. PM macro-components were grouped in order to evaluate the contribution of the main macro-sources (SOIL, SEA, SECONDARY INORGANIC, ORGANICS and TRAFFIC) and the analysis of the modulation of their concentration was found to strongly affects the absorption capability of the atmosphere over Rome. The surface forcing efficiency, provided by the decreasing trend of UV index with AOD, which is the primary parameter affecting the surface irradiance, was found very significant, probably masking the dependence of UV index on SSA and Ångström exponents. Moreover it was found greater for larger particles and with a more pronounced slope at the smaller solar zenith angle. In Rome large particles are generally less absorbing since related to the presence of SOIL and SEA components in the atmosphere. The former contribution was found much higher in summer months because of the numerous episodes of Saharan dust transport

https://doi.org/10.5194/amt-2019-300
Preprint. Discussion started: 2 October 2019

1. Introduction

The aerosol influence on the incoming and outgoing solar radiation is a widely studied topic because of its relation with the Earth's radiative balance and climate. The aerosol influence on ultraviolet (UV) solar irradiance is also very important, particularly in urban areas, nevertheless still uncertain. In fact, the aerosol capability of absorbing UV radiation has important implications for tropospheric photochemistry, human health, and agricultural productivity (Dickerson et al., 1997; He and Carmichael, 1999; Castro et al., 2001; Casasanta et al., 2011; Mok et al. 2018).

The aerosol single scattering albedo (SSA), that is the ratio of the aerosol scattering to extinction coefficient, representing an index of the aerosol absorption capability, and the optical depth (AOD), are important radiative parameters to determine the aerosol effect on the UV irradiance at the surface.

Reuder and Schwander (1999) demonstrated that more than 80% of the aerosol effect on surface UV radiation due to increasing turbidity of the atmosphere can be estimated through aerosol optical depth and single scattering albedo.

UV absorption by aerosol, characterized by low SSA values at wavelengths shorter than 400 nm, is commonly attributed to organic aerosols that absorb predominantly in the UV region and show a stronger wavelength dependence than a purely black carbon absorption (Kirchstetter et al., 2004). Also mineral components shows a significant absorption in the UV region, as highlighted by Meloni et al. (2006).

Martins et al. (2009) indicated that the absorption efficiency of urban aerosol is considerably larger in the UV than in the visible and is probably linked to the absorption by organic aerosol. Similarly, an enhancement of aerosol absorption at UV wavelengths was observed in urban cities such as Rome, Italy (Ialongo et al., 2010) and Athens, Greece (Kazadzis et al., 2016), especially in winter.

di Sarra et al. (2002), Panicker et al. (2009), and Antón et al. (2011), among others, have shown that an increase of AOD induces a reduction of the UV index (UVI), an effective parameter to quantify the potentially harmful effects of UV radiation. These studies suggested that a unit increase in aerosol optical depth at about 400 nm may produce a significant decrease of UVI which depends on the solar zenith angle and aerosol properties, and may exceed 50%.

This work is aimed at determining for the first time the effect of aerosol optical properties retrieved in Rome on UV radiation, evaluating the role of SSA, AOD and Ångström exponent. The dataset covers the period from March to September of 6 years, from 2010 to 2016. Only Spring and Summer periods were selected, when solar zenith angles smaller than 40° and then higher values of UVI can be analyzed. For SZA>40, as in winter time, the UV index is low, and shows a little range of variability during the day. Therefore the estimation error of UV index, that is about 4-5%, (Schmalwieser et al., 2017) could affect the identification of its variation due to possible aerosol effect. , Aerosol optical properties were

https://doi.org/10.5194/amt-2019-300
Preprint. Discussion started: 2 October 2019

Atmospheric Measurement Techniques Discussions

provided by a PREDE-POM sun-sky radiometer of the ESR/SKYNET (www.euroskyrad.net) network, and the UV index values were measured by a Brewer spectrophotometer.

2. The site and Instruments

Rome is a large urban site, with about 3 million inhabitants, located 25 km east of the Tyrrhenian Sea, in the middle of an undulating plain. The atmosphere is affected by urban emissions as well as by semi-rural particulates and, especially during the summer season, by sea breeze and long-range desert dust advection from the Saharan region (e.g., Ciardini et al., 2012).

Long term measurements of aerosol physical and optical properties, columnar ozone content and UV irradiance (290 -325 nm) are carried out in Rome, on the roof of the Physics Department of Sapienza University (41.9°N, 12.5°E; altitude 60 m) at the Laboratory of Geophysics. This site is located in the central sector of the city.

Aerosol properties are retrieved by the observations taken in clear sky conditions by the sun-sky radiometer PREDE/POM model 01, (hereafter called POM), a narrow band filter photometer able to perform measurements of direct solar and diffuse sky irradiances at selected wavelengths (315, 400, 500, 675, 870, 940 and 1020 nm) and at 24 scattering angles, in the range [0 –180°] in the almucantar geometry. The 315 and 940 nm channels are used to retrieve ozone and water vapour columnar content, whereas the other ones provide information on aerosols. The time resolution is 1 minute for direct irradiance and 10 minutes for diffuse irradiances. This instrument is part of the European Skynet Radiometer network (ESR, Campanelli et al., 2012; www.euroskyrad.net) that is a regional subnetwork of SKYNET (Takamura et al:, 2004); it has been operating in Rome since 2010 up to present. Calibration is performed monthly by the Improved Langley method (Campanelli et al., 2007), a well-tested "on-site" procedure that allows to frequently check the instrument status.

UV irradiance and total ozone content have been measured since 1992 at Rome by the Brewer Mk IV spectrophotometer No.067. This instrument is also operating by the Physics Department of Sapienza University at the Laboratory of Geophysics in Rome and is part of a European Brewer Network (EUBREWNET). The Brewer Mk IV is a single monochromator spectrophotometer specifically designed to retrieve through a well-defined data processing (Siani et al., 2018) the total column ozone by measuring solar direct irradiances at selected UV wavelengths in the ozone absorption spectrum (Kerr et al., 1981). The accuracy of direct-sun measurements of total ozone taken with a well-maintained Brewer spectrophotometer is 1% (Vanicek, 2006). The performance of the Brewer instrument for UV measurements was controlled every two years till 2014 through intercomparisons to the traveling reference QASUME UV spectroradiometer operated by Physykalish Meteorologisches Observatorium

https://doi.org/10.5194/amt-2019-300
Preprint. Discussion started: 2 October 2019

Davos/ World Radiation Centre. The mean ratio of Brewer integrated solar UV irradiances to QASUME is within +3% (see https://www.pmodwrc.ch/en/world-radiation-center-2/wcc-uv/). After that the UV calibration has been carried out by IOS using 1000w lamps which are traceable to the QASUME reference spectroradiometer (Siani, et al:, 2013). The Brewer also measures global spectral irradiances from 290 nm to 325 nm with a spectral resolution of about 0.5 nm at 0.5 nm steps. UV spectral scans are performed at Rome every 30 min throughout the day. The Brewer algorithm for the spectral interval 325 -400 nm assigns a higher weight to the measurement at 324 nm wavelength to compensate for the missing contribution of wavelengths longer than 325 nm. It has been found that this interpolation method introduces an error typically <2% in the UV index value for solar zenith angles <70°. (Fioletov et al., 2004).

To complete the characterization of aerosol properties at Rome during summer, results from an intensive field campaign (URBan Sustainability Related to Observed and Monitored Aerosol – URBS ROMA, Campanelli et al., 2012) conducted in the period June – July 2011 in the same location and aimed to determine the aerosol direct radiative effect at the surface, were used. Particulate matter 10 micrometers or less in diameter (PM10) mass concentrations were collected by using a dual channel sampler (HYDRA Dual Sampler, FAI Instruments, Fonte Nuova, Rome, IT) equipped with Teflon membrane filters and quartz fiber filters on the two channels, and PM10 mass concentration was measured on Teflon filters by gravimetry using an automated microbalance.

The elastic Lidar of the Sapienza University was also operative simultaneously with the other instruments and, in this study, it was used to discriminate days affected by desert dust.

Finally, during the period under analysis, the following ancillary meteorological parameters have also been used: atmospheric pressure provided by the Agenzia Regionale per la Protezione Ambientale (ARPA – Lazio), and cumulated precipitation measured at the station Roma Macao of the Ufficio Idrografico e Mareografico of Rome, less than 1 km far from the Department of Physics of Sapienza University.

3. Methodology

The POM normalized radiance (that is the radio between the solar diffuse radiance and direct solar irradiance) is inverted using the Skyrad4.2 pack (Nakajima et al., 1996), which is an official computer code of the SKYNET network. Signals from the channels centered at the wavelengths of 400, 500, 675, 870, and 1020 nm are analyzed in order to determine AOD, SSA, and Ångström exponent (Ang), the latter obtained by using all the wavelengths. In addition, the Ångström exponent is also calculated from the AOD at 400 and 500 nm ($Ang_{400-500}$) to infer the AOD wavelength dependence in the spectral range

https://doi.org/10.5194/amt-2019-300
Preprint. Discussion started: 2 October 2019

closest to the UV region. Cloud screening and quality check of the retrieved inversions are also performed. The cloud screening is based on the direct solar irradiance variability in 3 minute time interval, as explained in Estelles et al. (2012); the quality check of SSA and AOD at 400 nm (SSA_{400}, and AOD_{400}, respectively), that is the POM shortest wavelength used in this analysis, is based on the results from the most recent literature on Skyrad pack. Hashimoto et al. (2012) performed numerical tests on the SSA_{400} retrievals using the Rstar-6b radiative transfer code (Nakajima and Tanaka, 1986) and Skyrad pack (versions 4.2 and 5.0) inversions. They obtained SSA_{400} values of about 0.70 for dust-like and water insoluble aerosol models. A cirrus contamination case, obtained by enhancing the coarse mode for simulating the presence of ice particle types, according to the cirrus particles model of the World Climate Programme report (Deepak and Gerber, 1983), provided values varying between 0.71-0.75. Therefore, in this study measurements of SSA_{400} lower than 0.70 were rejected even if values between 0.70 and 0.75 could contain information on dust presence during possible cloud contaminated cases. Hashimoto et al. (2012) also demonstrated that the SSA retrieval by Skyrad4.2 pack is problematic, since sometimes SSA tends to be unnaturally close to unity, irrespectively of the AOD. Therefore, inversions where SSA_{400} assumed values ≥ 0.99 were also rejected. In this work we used only SSA at 400 nm as absorption estimation parameter because the comparison against retrievals from other versions of the Skyrad code showed good agreement at this wavelength and discrepancies at the others.

The UVI was introduced in Canada in 1992 (Fioletov, 2010) to represent the potentially harmful effects of UV radiation in a simple form. UVI is a unit-less quantity determined by multiplying the erythemally weighted UV irradiances (in W m^{-2}) over the range 280-400 nm by 40 m^2W^{-1} (Cost -713, 2000). UVI values are grouped into exposure category expressing the risk for unprotected skin to Sun exposure. Typically at mid-latitudes, UVI values at noon vary from 0 to 10, but highest UVI values were experienced at high altitude (e.g., Casale et al., 2015) and lower latitude sites. Spectral UV irradiances measured by the Brewer spectrophotometer in clear sky conditions (no clouds over the sun) were used to retrieve UV index values. The spectral irradiances were processed using the SHICrivm software (version 3_075) to obtain the biologically effective UV irradiance by weighting the solar irradiances with a function (action spectrum) representing the effectiveness of UV radiation to produce the erythemal response in the skin (C.I.E., 1998). The SHICrivm software was also applied to check for any spectral wavelength shift and spectral anomalies (Slaper et al, 1995) in the UV data. In addition, since the Brewer MKIV spectrophotometer measures spectral irradiances up to 325 nm, the non-measured part of the UVA spectrum needed for the calculation of UVI was also extrapolated by the same software.

Total ozone values (O_3) from direct-sun measurements were generated by using Brewer Processing Software, applying the rejection criteria on ozone values less than 100 DU and greater than 500 DU

https://doi.org/10.5194/amt-2019-300
Preprint. Discussion started: 2 October 2019

(Siani et al., 2018). Yet, individual total ozone values were discarded when standard deviation is above 2.5 DU and ozone air mass (defined as the ratio of the actual ozone path length taken by the direct solar beam to the analogous vertical ozone path when the Sun is overhead from the surface to the top of the atmosphere) is above 3.5.

To discern the dependence of UVI only on aerosol characteristics, the UVI dependence on the solar zenith angle (θ), ozone content, and orbital parameters (varying Earth-Sun distance) must be taken into account. Therefore, firstly the UVI was corrected for the variation of the Earth-Sun distance and values were reduced to the mean Sun-Earth distance (Madronich, 1993). Secondly, only data at two values of θ, 30° and 40°, were selected. This criterion excludes winter data, when the solar zenith angle is always higher than 40° in Rome. Thirdly, the UVI dependence on total O_3 has been removed. This correction has been implemented using the Radiation Amplification Factor (RAF) and scaling the UVI to the total ozone value measured during the day with the lowest AOD_{400} recorded in the entire dataset (303 DU on September 2, 2014). Infact the effect of ozone on the erythemal UV irradiance may be described as suggested by Madronich (1993) and Booth and Madronich (1994):

$$\frac{E^*}{E} = \left(\frac{O_3}{O_3^*}\right)^{RAF}, \qquad (1)$$

where E and E* are two UV irradiances observations, and O_3 and O_3* their corresponding total ozone amounts.

Similarly, it is possible to apply the above relationship to UVI:

$$UVI^* = UVI\left(\frac{<O_3>}{O_3^*}\right)^{RAF} , \qquad (2)$$

where <O_3> is the diurnal ozone average value, O_3* is the diurnal ozone average value during the day with the minimum average AOD_{400}, and RAF is assumed to be equal to 1.25, according to di Sarra et al. (2002). To point out the possible effect of aerosol optical characteristics measured at 400 nm on UVI^*, AOD_{400}, SSA_{400}, Ang and $Ang_{400\text{-}500}$ were analyzed as function of UVI^* at the two fixed solar zenith angles, taking estimations of aerosol parameters and UVI* within ±5 minutes.

Chemical characterization of the collected PM10 dust, during the URBS campaign, was carried out according to the method reported in Perrino et al. (2009). Briefly, elements were determined on Teflon filters by X-ray fluorescence (XRF); then the filters were water-extracted and analyzed for their ionic content by ion chromatography (IC); elemental and organic carbon (EC and OC) were detected on quartz filters by thermo-optical analysis (NIOSH-QUARTZ temperature protocol). This overall analytical procedure allows the determination of each individual component typically accounting for more than

https://doi.org/10.5194/amt-2019-300
Preprint. Discussion started: 2 October 2019

1% of the mass amount of PM10 (macro-components: Si, Al, Fe, Na, K, Mg, Ca, chloride, nitrate, sulfate, ammonium, elemental carbon, organic carbon) and to obtain the mass closure.

PM10 macro-components can be grouped into five clusters to estimate the contribution of the main macro-sources: SOIL, SEA, SECONDARY INORGANICS, ORGANICS, and TRAFFIC. Details about the algorithms are reported in Perrino et al. (2014). Briefly, the contribution of SOIL was calculated by adding the concentration of elements (as metal oxides) generally associated with mineral dust: Al, Si, Fe, the insoluble fractions of K, Mg, and Ca (calculated as the difference between XRF and IC determinations), calcium and magnesium carbonate (calculated as the sum of soluble calcium multiplied by 1.5 and soluble magnesium multiplied by 2.5); SEA was estimated from the sum of Na^+ and Cl^-, multiplied by 1.176 in order to take into account minor sea-water components; SECONDARY INORGANICS were calculated as the sum of non-sea-salt sulphate, nitrate, and ammonium; the contribution of road TRAFFIC was estimated by adding elemental carbon to an equivalent amount multiplied by 1.1 in order to consider the contribution of primary organic matter that can be adsorbed on particles surface; the remaining organic carbon, multiplied by 1.6 to take into account non-C atoms, constituted the ORGANICS and included both secondary organic species and primary components.

4. Results

The analyzed dataset covers the period March – September from 2010 to 2016 (for the last year the series end in August). Figure 1 shows monthly average SSA_{400}, AOD_{400}, and Ångström exponent for the period under examination. Annual means (calculated over the 7 months under study) of SSA_{400} vary between a minimum value of 0.84±0.08 (observed in 2016) and a maximum of 0.97±0.03 (observed in 2015); the large SSA decrease in 2016 is also observed by AERONET estimates of SSA at 440 nm (shown with red points in Figure 1), obtained from measurements taken in TorVergata, a semirural area 14 km south east of the town. The AERONET inversion is performed according to Dubovik and King (2000) and it is able to retrieve aerosol optical properties from Sun and sky radiance measurements. In this study we used level 1.5 data and Version 3 inversion algorithm (Giles et al., 2019). Although the two sites are slightly different in terms of atmospheric particles optical properties, and the wavelength used for AOD, SSA and Ångström differs, the agreement between the AERONET and SKYNET properties for the 3 common months in 2016 is significant and the decreasing trend in SSA is visible from AERONET inversion. The decrease is even stronger from March to May. However, we are not able to identify the reason for this enhanced aerosol absorption. AOD_{400} mean values range between a minimum of 0.14±0.06 (in 2014) and a maximum of 0.36±0.10 (in 2015; values higher than 0.3 are measured only in this year for the period under study). The Ångström exponent varies between 0.56±0.29 (in 2012) and 1.49±0.21 (in 2011). The total ozone content values and UVI at local noon are also plotted in Figure.1.

The seasonal ozone behavior is typical of mid-latitude sites, with highest values measured in 2010 and 2016. As expected, UVI has a bell-shape behavior generally peaked in July. The monthly cumulated precipitation and the monthly average atmospheric pressure are also plotted in the same figure.
Scatter plots of monthly average AOD_{400}, SSA_{400}, Ang, and UVI versus monthly precipitation (Figure. 2) were performed in order to check if precipitation can affect on average the optical parameters.
The only two parameters showing a slight correlation are SSA_{400} (R=0.30) and UVI (R= -0.60), highlighting that higher precipitation is associated with higher values of SSA (therefore less absorbent particulate) and with lower UVI values. These correlations among monthly mean values may be incidental, or due to the combination of different processes. In particular, we may expect that a higher occurrence of scattered clouds conditions, corresponding to lower UVI values, may be associated with periods with high precipitation during short-lived weather spring-summer disturbances. Possible effects on SSA_{400} may be linked to the possible influence of high humidity conditions, leading to a larger water content in soluble particles. This is however speculative, and a detailed analysis goes beyond the scope of this paper.
During June-July 2011 the chemical analysis of the collected PM10 (Figure 3) measured an average contribution over the entire mass of about 29% of SOIL, 6% of SEA, 23% of SECONDARY INORGANIC, 28% of ORGANICS and 9% of TRAFFIC components. During the URBS- ROMA campaign, the elastic Lidar showed the presence of significant events of desert dust transport, the strongest observed during the days highlighted in orange in Figure 3. It must be considered that in the days flagged as "dusty", dust can remain at a higher level and not measurable at ground (this is the case of 3 and 18 July). Conversely, sometimes a lot of aerosol is visible at ground level but it was not possible discriminating the presence of desert dust from the local SOIL component (this is the case of July 2 and 17).. The atmosphere over Rome, during summer, generally is characterized by a contribution of SEA comparable with the TRAFFIC, or even greater during days with no desert dust advection. The absorption capability of these two components is very different: in the Rstar radiative transfer model (Nakajima and Tanaka 1986), at 413 nm the imaginary part of marine aerosol refractive index is $2.42x*10^{-8}$, whereas for soot, that is the fundamental material characterizing the TRAFFIC component, is $4.57x10^{-1}$. The mineral component has a refractive index of $7.95x10^{-3}$ at the same wavelength. It is therefore expected that modulation of the concentration of the three co-existent materials, can strongly affect the absorption capability of the atmosphere over Rome.

https://doi.org/10.5194/amt-2019-300
Preprint. Discussion started: 2 October 2019

Atmospheric Measurement Techniques
Discussions

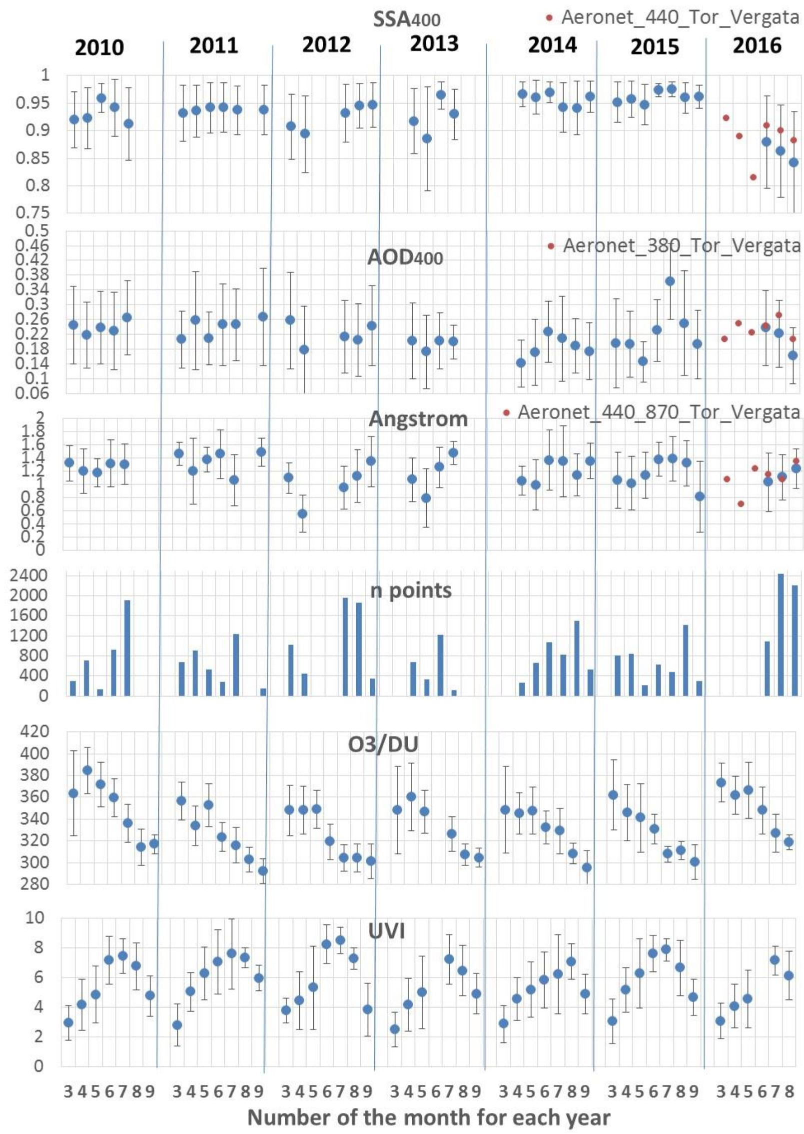

267

268

269 Figure 1: Monthly averages of SSA_{400}, AOD_{400}, Ångström exponent, cumulated precipitation, total O_3,

270 UVI, and atmospheric pressure for each year from 2010 to 2106. The number of points refers to the data

271 used to retrieve the aerosol parameters. Error bars are the standard deviation.

https://doi.org/10.5194/amt-2019-300
Preprint. Discussion started: 2 October 2019

Atmospheric Measurement Techniques
Discussions

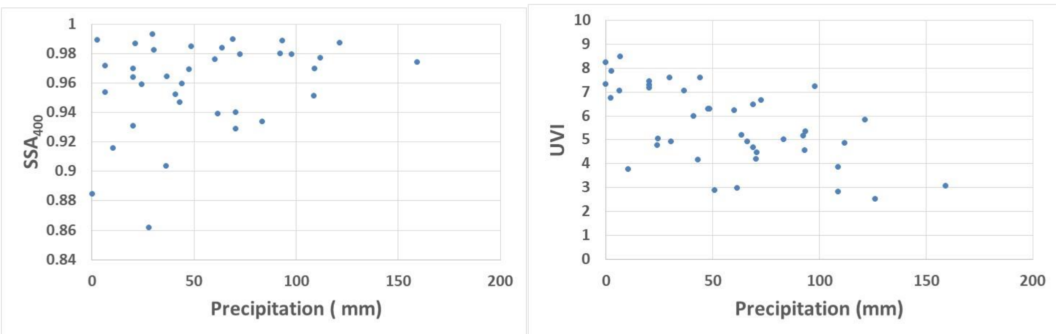

Figure 2: monthly average of SSA_{400} (left) and UVI (right) versus monthly precipitation

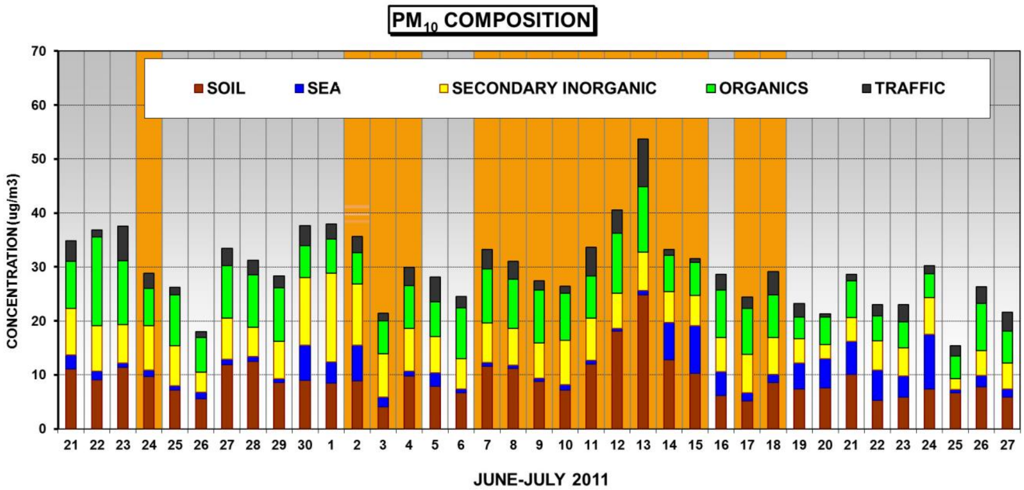

Figure 3: Concentration of the components of PM10 collected in Rome from 21 June to 27 July 2011 as derived from chemical analyses. Orange columns represent days affected by the passage of desert dust, as measured by Lidar.

A statistical analysis of daily means of SSA_{400}, AOD_{400} and Ångström exponent with the percentage contribution of each chemical component, has been performed in order to connect optical properties and chemical analysis. In fact, assuming that the in situ measurements are representative of the entire column, their variation affects particles refractive index and particles dimensions, and consequently their absorption capability and Ångström exponent. Scatter plot of SSA_{400} versus the SOIL component (Figure 4) shows a slight negative correlation (R= -0.54), whereas no other correlation is visible for the other components and other optical and physical parameters. This result underlines that in situ

https://doi.org/10.5194/amt-2019-300
Preprint. Discussion started: 2 October 2019

Atmospheric Measurement Techniques Discussions

measurements may not provide information correlated with the columnar properties, because optical and physical properties at the ground may differ from those of the entire column. Therefore, both information must be used complementarily for understanding the radiative effects of such a mixture of different components.

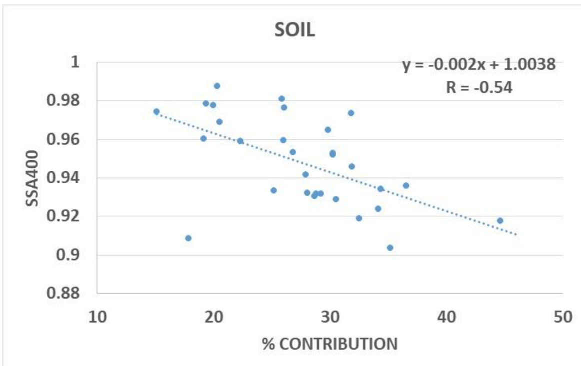

Figure 4. Behaviour of SSA_{400} versus the percentage contribution of SOIL component as retrieved during the URBS campaign.

Assuming that relations between aerosol composition and their optical properties, measured during summer 2011, are comparable in the last years, they can be considered as representative of the summer period 2010-2016 studied in this paper.

In order to point out the possible effect of aerosol optical characteristics measured at 400 nm on UVI^*, the AOD_{400}, SSA_{400}, Ang, and $Ang_{400-500}$, were analyzed as function of UVI^*, at the two selected values of solar zenith angle. Figure 5 shows the frequency distributions of the number of measurements for each of the two angles. θ=30° is more representative of the warmest months, whereas 40° covers a wider period.

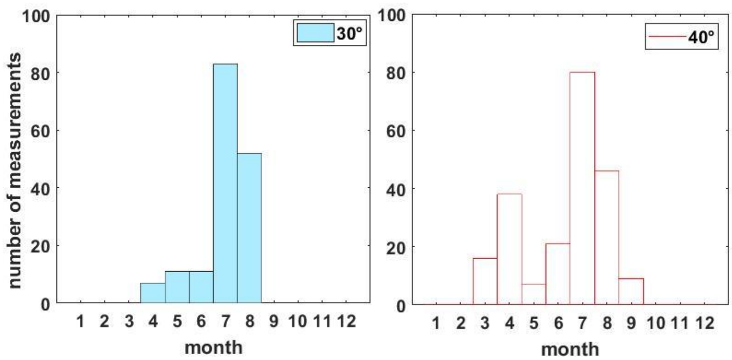

Figure 5: Number of measurements available for each zenith angle.

https://doi.org/10.5194/amt-2019-300
Preprint. Discussion started: 2 October 2019

The dependency of UVI^* on AOD_{400}, SSA_{400}, Ang and Ang_{400_500} for 30° and 40° solar zenith angles are shown in Figure 6, colored for different values of SSA_{400} or AOD_{400}. A clear linear decreasing trend of UVI^* when increasing AOD_{400} is evident. The slope in these graphs corresponds to the UVI* radiative forcing efficiency, i.e., the change in UVI* produced by a unit change in AOD. The slope is more pronounced at the smaller solar zenith angle (Table I), as already found by previous studies (di Sarra et al., 2008; Antón et al., 2011). No clear dependence of UVI^* on SSA_{400} or on Ångström exponents can be noticed. If existent, it is expected to be masked by the dependency on AOD, which is the primary parameter affecting the surface irradiance.

To investigate in more detail, the entire dataset was divided in three groups of Ang_{400_500}, below 0.8, between 0.8 and 1.7, and above 1.7, and in two groups of SSA_{400}, smaller and larger than 0.85, respectively. The values separating the different groups were determined according to the frequency distributions of the two variables for the entire investigation period, shown in Figure 7. Scatter plots and linear fits of UVI* versus the two variables, for each group, were performed and points with a distance greater than 2σ from the regression line (nout), with σ the standard deviation of the residuals, were rejected.

The dependence of UVI^* on AOD for the three classes of $Ang_{400-500}$ is shown in Figure 8, colored for different values of SSA_{400}, and in Table I. The slope is generally larger for smaller values of $Ang_{400-500}$, similarly to what found by Antón et al. (2011). At 30° the other two classes of $Ang_{400-500}$ have a very similar slope, differing of 0.15 that is below its uncertainty estimation from the fit. Conversely at 40° an intermediate value of the slope is found for $Ang_{400-500} \geq 1.7$; this value appears essentially driven, for both the zenith angles, by cases with low SSA and low AOD, which might be attributed to a possible influence from combustion particles characterized by small size and high absorption (see, e.g., Pace et al., 2005). A similar dependency on the Ångström exponent was found by di Sarra et al. (2008) when considering the forcing efficiency over the whole shortwave spectral range. The smallest slope is associated to the $0.8<Ang_{400-500}\leq 1.7$, range which is characterized by a larger mixture of absorption capabilities.

The Ångström exponent in Rome varies between about 0.5 and 1.8 (Figure 7), with a typical range of variability of 1.3. The estimated effect of the Ang variability can be determined by considering the slope difference among the different values of Ang, which is of the order of 1.5 at 30° solar zenith angle. The corresponding change of UVI* is about 2.

Figure 9 shows the scatter plots of UVI^* vs AOD_{400} for SSA_{400} <0.85 (left side) and $SSA_{400} \geq 0.85$ (right side), with a colour scale for different values of the Ångström exponent at the two zenith angles.. For solar zenith angles 30° (Table II) the slope of UVI^* versus AOD_{400} is larger for $SSA_{400}\geq 0.85$, increasing

https://doi.org/10.5194/amt-2019-300
Preprint. Discussion started: 2 October 2019

Atmospheric Measurement Techniques Discussions

of about 67% going from -1.77 to -2.96. This increase is significant, since it is greater than the uncertainty of the estimated slope. For solar zenith angles 40° the increase is about 9%, going from -1.42 to -1.55, but in this case it is comparable with the estimated uncertainties of the slope, varying from 15% for SSA_{400} <0.85, to 7% for $SSA_{400} \geq 0.85$. This result is opposite to what Antòn et al. (2011) found in Granada, Spain, where, as expected, stronger aerosol absorption leads to a large surface forcing efficiency.

Looking at the UVI* versus AOD_{400} or the UVI* versus SSA_{400} scatter plots in Figure 6 it is evident that for both solar zenith angles (but mostly at the smaller one) less absorbing particles (higher SSA_{400}) correspond to higher AOD_{400}. This is also confirmed by the mean and median AOD_{400} values calculated over all the years in the months analyzed in Rome (Table III) with the additional information that higher AOD_{400} are also characterized by greater particles ($Ang_{400\text{-}500} < 0.8$). This is probably due to the presence of SOIL and SEA salt in the atmosphere, as highlighted during URBS.

As shown in Figure 7, SSA varies between about 0.75 and 1.0, for a variability range of 0.25. The slope difference among the different values of SSA about 1, and a rough estimate of the corresponding change of UVI* is of about 0.25. This value is much smaller than the expected effect produced by Ang that is a change of about 2. Thus, it is very likely that the effect of variations of single scattering albedo may be masked by concomitant changes of Ang.

θ=**30°**	Slope (m)	Intercept (q)	R	θ=**40°**	Slope (m)	Intercept (q)	R
$Ang_{400\text{-}500} < 0.8$	-3.73±0.31	8.04	-0.96	$Ang_{400\text{-}500} < 0.8$	-2.46±0.34	6.00	-0.87
$0.8 \leq Ang_{400\text{-}500} < 1.7$	-2.28±0.24	7.82	-0.77	$0.8 \leq Ang_{400\text{-}500} < 1.7$	-1.38±0.11	5.68	-0.78
$Ang_{400\text{-}500} \geq 1.7$	-2.13±0.37	7.76	-0.78	$Ang_{400\text{-}500} \geq 1.7$	-1.62±0.24	5.62	-0.83

Table I: The slope, intercept and correlation coefficient for the linear fit of UVI* vs AOD_{400}, in three cases: data selected for $Ang_{400\text{-}500} < 0.8$; $0.8 \leq Ang_{400\text{-}500} < 1.7$; $Ang_{400\text{-}500} \geq 1.7$, for the two zenith angles

θ=**30°**	Slope (m)	Intercept (q)	R	θ=**40°**	Slope (m)	Intercept (q)	R
All data	-1.97±0.21	7.80	-0.65	All data	-1.36±0.14	5.68	-0.60
SSA_{400}<0.85	-1.77±0.21	7.71	-0.77	SSA_{400}<0.85	-1.42±0.22	5.61	-0.73
SSA_{400}≥0.85	-2.96±0.21	8.17	-0.89	SSA_{400}>0.85	-1.55±0.11	5.76	-0.82

Table II: slope, intercept and correlation coefficient for the linear fit of UVI* vs AOD_{400}, in three cases: all the dataset, data selected for SSA_{400}<0.85 and SSA_{400}≥0.85 for the two zenith angles.

https://doi.org/10.5194/amt-2019-300
Preprint. Discussion started: 2 October 2019

Atmospheric Measurement Techniques Discussions

	AOD_{400} at θ=**30°**		AOD_{400} at θ=**40°**	
	Mean ± std	median	Mean ± std	median
SSA_{400}<0.85	0.186±0.099	0.185	0.200±0.095	0.187
SSA_{400}≥0.85	0.296±0.118	0.274	0.262±0.135	0.249
Ang400_500<0.8	0.345±0.134	0.330	0.218±0.129	0.174
Ang400_500>=1.7	0.117±0.066	0.105	0.155±0.088	0.124

Table III: mean and median AOD_{400} values calculated over all the years in the months analyzed in Rome, separately for different classes of SSA and Ang.

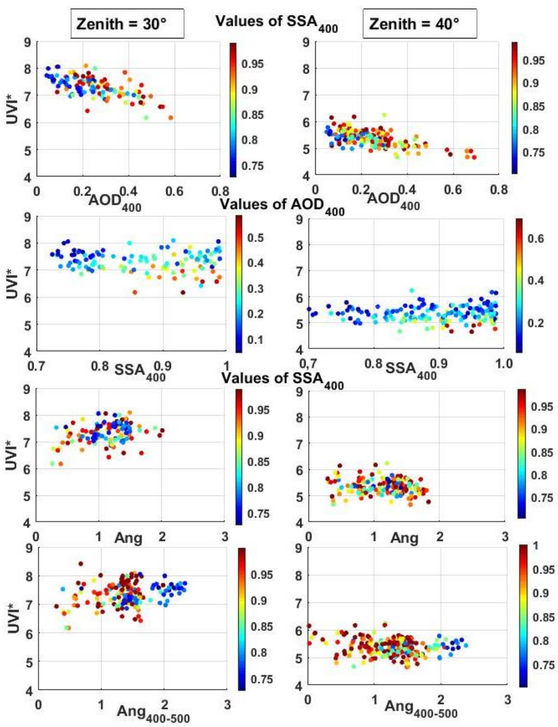

Figure 6. Scatter plot of UVI* vs AOD_{400} (top), SSA_{400} (middle), and Ang and $Ang_{400\text{-}500}$ (bottom) for the solar zenith angles of 30° (left) and of 40° (right). The colors represent the values of SSA_{400} (first, third and fourth rows) and AOD_{400} (second row).

https://doi.org/10.5194/amt-2019-300
Preprint. Discussion started: 2 October 2019

Atmospheric Measurement Techniques
Discussions

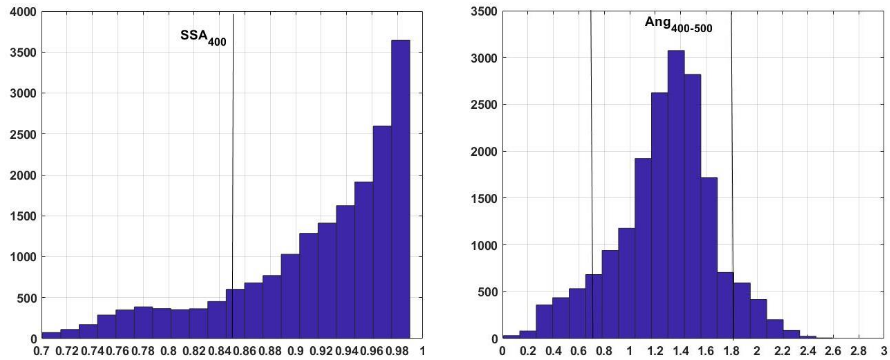

Figure 7. Frequency distributions of SSA_{400} (left) and $Ang_{400-500}$ (right) for the entire investigation period. The threshold values separating the different classes are highlighted with vertical black lines.

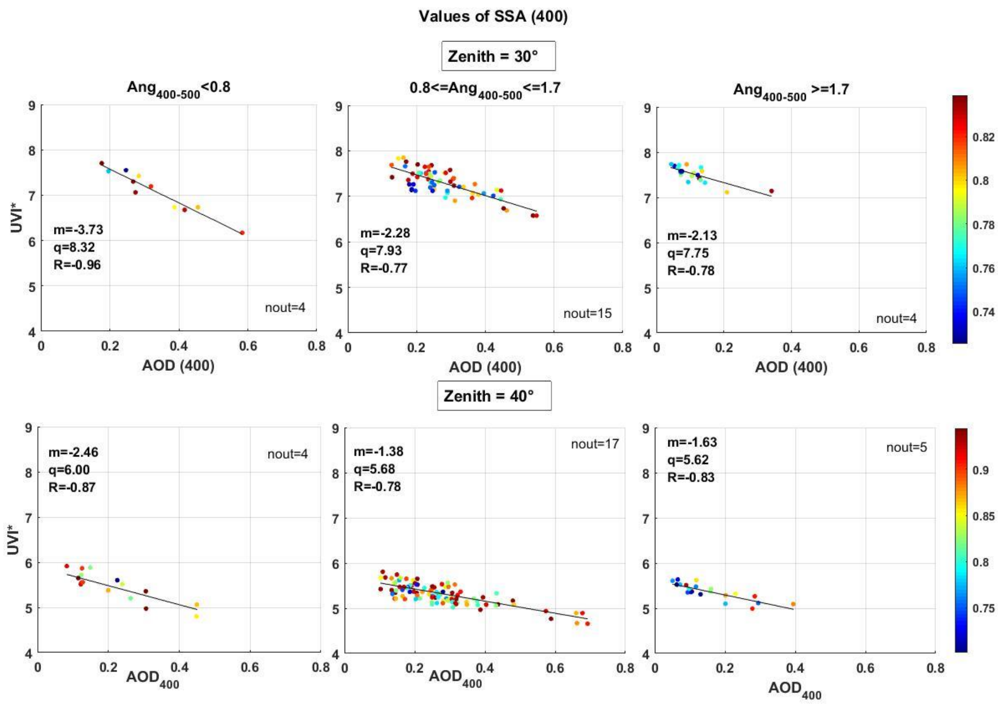

Figure 8: scatter plot of UVI* vs AOD_{400} for three groups of $Ang_{400-500}$ (left, middle, right) and two solar zenith angles (top, bottom). The colors represent the values of SSA_{400}. nout is the number of rejected outliers.

https://doi.org/10.5194/amt-2019-300
Preprint. Discussion started: 2 October 2019

Atmospheric Measurement Techniques
Discussions

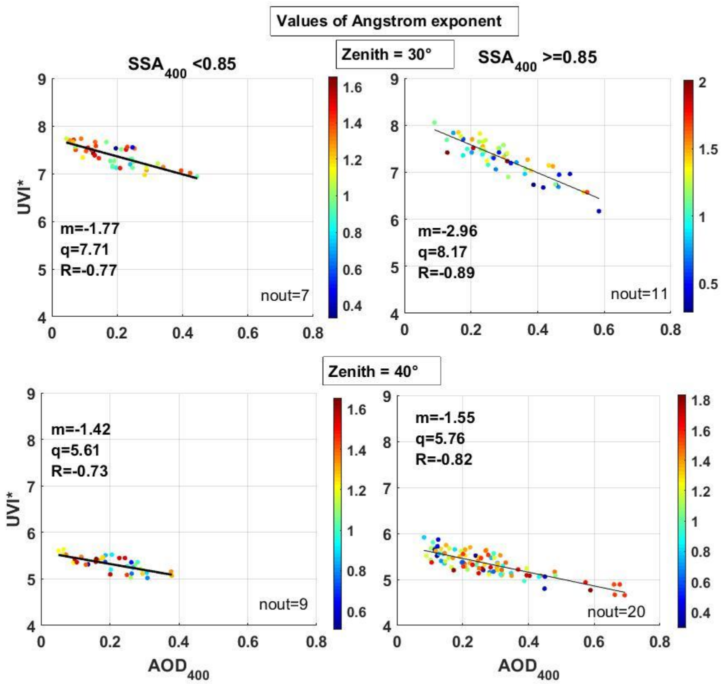

Figure 9: scatter plot of UVI* vs AOD400 for two groups of SSA400 (right and left) and two solar zenith angles (top and bottom). The colour scale refers to the values of Ang. nout is the number of rejected outliers.

5. Conclusions

The aerosol optical characteristics in the urban area of Rome were retrieved for a period of 7 years, in the months from March to September 2010-2016. The impact of SSA, AOD at 400 nm, and Ångström exponent on the UV index has been analyzed. The evolution of UVI*, which is the measured UV index corrected for total ozone changes and scaled at the mean Sun-Earth distance, was studied d with respect to AOD_{400}, SSA_{400}, and Ångström exponent calculated using all the wavelengths (Ang) and only AOD at 400 and 500 nm. Data at two fixed values of the solar zenith angle were selected in order to point out the possible effect of aerosol optical characteristics measured at 400 nm on UVI^*.

A clear linear decreasing trend of UVI* when increasing AOD_{400} was found, with a more pronounced slope at the smaller solar zenith angle, as already shown by previous studies. The dependence of UVI^* on SSA_{400} and Ångström exponents is probably masked by the dependency on AOD, which is the primary parameter affecting the surface irradiance. The entire dataset was also analyzed separately for different absorption properties (by fixing a threshold value for SSA_{400}) and for different aerosols dimensions (by fixing threshold values for $Ang_{400-500}$). The surface forcing efficiency, provided by the decreasing trend of UVI* with AOD_{400}, was found greater for larger particles. In Rome these particles, having small Ångström exponent values, are generally less absorbing since related to the presence of SOIL and SEA components in the atmosphere. Moreover the former contribution is much higher in summer months (as highlighted from the chemical characterization of suspended particulate matter over Rome during the URBS ROMA intensive field campaign held in 2011) because of the numerous episodes of Saharan dust transport. The result is that the effect of the Angstrom exponent on the incoming UV radiation could mask the dependence on the SSA.

The general behavior observed for the five macro-sources (SOIL, SEA, SECONDARY INORGANIC, ORGANICS and TRAFFIC) during summer 2011 has been assumed not substantially changed in the last years, and the variations in the absorption capability of the atmosphere over Rome were attributed to the different absorption characteristics of the macro- components and their modulation of concentration in the atmospheric mixture.

A better understanding of the impact of aerosol optical properties in Rome on UVI* can be done in the next future using measurements of direct and diffuses solar radiation at 340 nm, instead of 400, available at the ESR Rome site from 2018. Also the use of different versions of the Skyrad code (as version 5.0) can improve the retrieval of the SSA wavelength dependence, making possible the calculation of the Absorption Ångström Exponent for a better characterization of the absorption properties.

6. Acknowledgements:

We thank Gian Paolo Gobbi and collaborators for establishing and maintaining the Rome–Tor Vergata AERONET site used in this investigation. We also thanks ARPA-LAZIO for providing meteorological data over Rome.

7. References

Antón, M., J. E. Gil, J. Fernández-Gálvez, H. Lyamani, A. Valenzuela, I. Foyo-Moreno, F. J. Olmo, and L. Alados-Arboledas, Evaluation of the aerosol forcing efficiency in the UV erythemal range at Granada, Spain, J. Geophys. Res. 116, D20214, doi:10.1029/2011JD016112, 2011

Campanelli, M., Estellés, V., Smyth, T., Tomasi, C., Martínez-Lozano, M. P., Claxton, B., Muller, P., Pappalardo, G.,Pietruczuk, A., Shanklin, J., Colwell, S., Wrench, C., Lupi, A.,Mazzola, M., Lanconelli, C., Vitale, V., Congeduti, F., Dionisi,D., and Cacciani, M.: Monitoring of Eyjafjallajoekull volcanic aerosol by the new European SkyRad users (ESR) sun–sky radiometernetwork, Atmos. Environ., 48, 33–45, 2012.

https://doi.org/10.5194/amt-2019-300
Preprint. Discussion started: 2 October 2019

Campanelli M., C. Bassani, M. Cacciani, A.M. Siani , C. Perrino , S. Canepari , A. Di Sarra, R. Salzano, G.P. Casasanta , C. Tirelli , and V. Estelles: Direct effect of aerosol on incident solar radiation at the surface as a function of aerosol mixtures measured in the center of Rome, Geophysical Research Abstracts, Vol. 14, EGU2012-4820, 2012, EGU General Assembly.

Campanelli, M., Estellés, V., Tomasi, C., Nakajima, T., Malvestuto, V., and Martiínez-Lozano, J. A.: Application of the SKYRAD Improved Langley plot method for the in situ calibration of CIMEL Sun–sky photometers, Appl. Optics, 46, 2688–2702, 2007.

Casale, G.R., Siani, A.M., Diémoz, H., Agnesod, G., Parisi, A.V., Colosimo, A. Extreme UV index and solar exposures at Plateau Rosà (3500ma.s.l.) in Valle d'Aosta Region, Italy, Science of the Total Environment, 512-513, 622-630, 2015.

Casasanta, G., A. di Sarra, D. Meloni, F. Monteleone, G. Pace, S. Piacentino, and D. Sferlazzo, Large aerosol effects on ozone photolysis in the Mediterranean, *Atmos. Environ.*, **45**, 3937-3943, 2011.

Castro, T., Madronich, S., Rivale, S., Muhlia, A., and Mar, B.: The influence of aerosols on photochemical smog in Mexico City, Atmos.Environ., 35, 1765–1772, 2001

Ciardini, V., Di Iorio T., Di Liberto L.,, Tirelli C., Casasanta G., di Sarra A., Fiocco G., Fuà D., Cacciani M. : Seasonal variability of tropospheric aerosols in Rome, Atmospheric Research, Vol 118, 15 Nov. 2012, Pages 205-214 https://doi.org/10.1016/j.atmosres.2012.06.026

C.I.E. (Commission Internationale de l'Eclairage). Erythema reference action spectrum and standard erythema dose. CIE S007E-1998. 1998. CIE Central Bureau, Vienna, Austria

COST-713 Action. UV Index for the Public. European, Communities. Brussels, 27, 2000.

Deepak, A. and Gerber, H. E. (Eds.): Report of the Experts Meeting on Aerosols and Their Climatic Effects, Williamsburg, Virginia,28–30 March 1983: WMO-ICSU WCP-55, World Meteorology, Organization, Geneva, Switzerland, 107 pp., 1983.

Dickerson, R. R., Kondragunta, S., Stenchikov, G., Civerolo, K. L.,Doddridge, B. G., and Holben, B. N.: The impact of aerosolson solar ultraviolet radiation and photochemical smog, Science,278, 827–830, https://doi.org/10.1126/science.278.5339.827,1997

Dubovik, O. and M. D. King, 2000: A flexible inversion algorithm for retrieval of aerosol optical properties from Sun and sky radiance measurements," J. Geophys. Res., 105, 20 673-20 696.

di Sarra A., M. Cacciani, P. Chamard, C. Cornwall, J. J. DeLuisi, T. Di Iorio, P. Disterhoft, G. Fiocco, D. Fua`, and F. Monteleone Effects of desert dust and ozone on the ultraviolet irradiance at the Mediterranean island of Lampedusa during PAUR II Journal of Geophysical Research, Vol. 107, No. D18, 8135, doi:10.1029/2000JD000139, 2002

di Sarra, A., G. Pace, D. Meloni, L. De Silvestri, S. Piacentino, and F. Monteleone, Surface shortwave radiative forcing of different aerosol types in the Mediterranean, Geophys. Res. Lett., 35, L02714, doi:10.1029/2007GL032395, 2008.

Estellés V., M. Campanelli, T.J. Smyth, M.P. Utrillas and J.A. Martinez-Lozano, AERONET and ESR sun direct products comparison performed on Cimel CE318 and Prede POM01 solar radiometers, *ACP 2012 12*, 11619–11630, 2012.

Fioletov, V. E., Kimlin, M. G., Krotkov, N., McArthur, L. J. B., Kerr, J. B., Wardle, D. I., Herman, J. R., Meltzer, R., Mathews, T. W., and Kaurola, J. (2004), UV index climatology over the United States and Canada from ground-based and satellite estimates, J. Geophys. Res., 109, D22308, doi:10.1029/2004JD004820.

Fioletov, V., J. B. Kerr, A. Fergusson, The UV Index: Definition, Distribution and Factors Affecting It. Can. J. Public Health 101(4):I5-I9,2010.

Frederick, J. E., E. K. Koob, A. D. Alberts, and E. C. Weatherhead, Empirical studies of tropospheric transmission in the ultraviolet: Broadband measurements, J. Appl. Meteorol., 32, 1883– 1892, 1993.
Reuder, J., and H. Schwander, Aerosol effects on UV radiation in nonurban regions, J. Geophys. Res., 104, 4065–4077, 1999

Giles, D. M. and Sinyuk, A. and Sorokin, M. G. and Schafer, J. S. and Smirnov, A. and Slutsker, I. and Eck, T. F. and Holben, B. N. and Lewis, J. R. and Campbell, J. R. and Welton, E. J. and Korkin, S. V. and Lyapustin, A. I., Advancements in the Aerosol Robotic Network (AERONET) Version~3 database -- automated near-real-time quality control algorithm with improved cloud screening for Sun photometer aerosol optical depth (AOD) measurements,Atmospheric Measurement Techniques, 12, 2019, 1, 169-209, https://www.atmos-meas-tech.net/12/169/2019/, DOI 10.5194/amt-12-169-2019.

Hashimoto, M., T. Nakajima, O. Dubovik, M. Campanelli, H. Che, P. Khatri, T. Takamura, and G. Pandithurai: Development of a new data-processing method for SKYNET sky radiometer observations, Atmos. Meas. Tech., 5, 2723–2737, 2012, www.atmos-meas-tech.net/5/2723/2012/, doi:10.5194/amt-5-2723-2012

He, S. and Carmichael, G. R.: Sensitivity of photolysis rates and ozone production in the troposphere to aerosol properties, J. Geophys. Res., 104, 26307–26324,https://doi.org/10.1029/1999JD900789, 1999

Ialongo, I., Buchard, V., Brogniez, C., Casale, G. R., and Siani, A.M.: Aerosol Single Scattering Albedo retrieval in the UV range:an application to OMI satellite validation, Atmos. Chem. Phys.,10, 331–340, https://doi.org/10.5194/acp-10-331-2010, 2010.

International Ozone Service (IOS): International Ozone Service Inc., http://www.io3.ca/ (last access: 1 September 2018) September 2018

Kazadzis, S., Raptis, P., Kouremeti, N., Amiridis, V., Arola, A.,Gerasopoulos, E., and Schuster, G. L.: Aerosol absorption retrieval at ultraviolet wavelengths in a complex environment, Atmos.Meas. Tech., 9, 5997–6011, https://doi.org/10.5194/amt-9-5997-2016, 2016.

Kerr, J. B., C. T. McElroy, and R. A. Olafson, Measurements of ozone with the Brewer spectrophotometer, in Proceedings of the Quadrennial International Ozone Symposium, edited by J. London, pp. 74–79, Natl. Cent. for Atmos. Res., Boulder, Colo, 1981.

Kinney, J. P., C. S. Long, and A. C. Geller, The Ultraviolet Index:A useful tool, Dermatol. Online J., 6(1), 2, 1981.

Kirchstetter, T. W., Novakov, T., and Hobbs, P. V.: Evidence that the spectral dependence of light absorption by aerosols is affected by organic carbon, J. Geophys. Res., 109, D21208, https://doi.org/10.1029/2004JD004999, 2004.

Liu, C., Chung, C. E., Yin, Y., and Schnaiter, M.: The absorption Ångström exponent of black carbon: from numerical aspects, Atmos. Chem. Phys., 18, 6259-6273, https://doi.org/10.5194/acp-18-6259-2018.

Madronich, S., The Atmosphere and UV-B Radiation at Ground Level. In: Young A.R., Moan J., Björn L.O., Nultsch W. (eds) Environmental UV Photobiology. Springer, Boston, MA, 1993

Madronich, S., 1993: UV radiation in the natural and perturbed atmosphere. Environmental Effects of Ultraviolet Radiation, Lewis, Boca Raton,Florida. 17-69, Booth, C & Madronich, Sasha. Radiation amplification factors: Improved formulation accounts for large increases in ultraviolet radiation associated with Antarctic ozone depletion. Antarctic Research Series. 62. 39-42. 10.1029/AR062p0039, 1994.

Martins, J. V., Artaxo, P., Kaufman, Y. J., Castanho, A. D., and Remer, L. A.: Spectral absorption properties of aerosol particles from 350–2500 nm, Geophys. Res. Lett., 36, L13810, https://doi.org/10.1029/2009GL037435, 2009.

Meloni, D., A. di Sarra, G. Pace, and F. Monteleone, Optical properties of aerosols over the central Mediterranean. 2. Determination of single scattering albedo at two wavelengths for different aerosol types, *Atmos. Chem. Phys.*, **6**, 715–727, 2006.

Mok, J., Krotkov, N. A., Torres, O., Jethva, H., Li, Z., Kim, J., Koo, J.-H., Go, S., Irie, H., Labow, G., Eck, T. F., Holben, B. N., Herman, J., Loughman, R. P., Spinei, E., Lee, S. S., Khatri, P., and Campanelli, M.: Comparisons of spectral aerosol single scattering albedo in Seoul, South Korea, Atmos. Meas. Tech., 11, 2295-2311, https://doi.org/10.5194/amt-11-2295-2018, 2018.

Nakajima, T. and M. Tanaka, Matrix formulation for the transfer of solar radiation in a plane-parallel scattering atmosphere. J. Quant. Spectrosc. Radiat. Transfer, 35, 13-2, 1986.

https://doi.org/10.5194/amt-2019-300
Preprint. Discussion started: 2 October 2019

Nakajima, T., Tonna, G., Rao, R., Boi, P., Kaufman, Y., and Holben, B., Use of sky brightness measurements from ground for remote sensing of particulate polydispersions. Applied Optics 35, 2672-2686, 1996.

Pace, G., D. Meloni, and A. di Sarra, Forest fire aerosol over the Mediterranean basin during summer 2003, J. Geophys. Res., 110, D21202, doi:10.1029/2005JD005986, 2005.

Panicker A. S.,G. Pandithurai, T. Takamura,and R. T. Pinker Aerosol effects in the UV-B spectral region over Pune, an urban site in India Geophysical Research Letters, Vol. 36, L10802, doi:10.1029/2009GL037632, 2009.

Perrino C., S. Canepari, M. Catrambone, S. Dalla Torre, E. Rantica, T. Sargolini: "Influence of natural events on the concentration and composition of atmospheric particulate matter" Atmospheric Environment, 43, 4766-4779, 2009.

Perrino C., M. Catrambone, S. Dalla Torre, E. Rantica, T. Sargolini, S. Canepari: "Seasonal variations in the chemical composition of particulate matter: a case study in the Po Valley. Part I: macro-components and mass closure" Environ. Sci. Pollut. Res. 21, 3999-4009, 2014.

Reuder J., H. Schwander Aerosol effects on UV radiation in nonurban regions First published: 01 February 1999 https://doi.org/10.1029/1998JD200072 Journal of Geophysical Research, Vol. 104, No. D4, Pages 4065-4077, February 27, 1999.

Schmalwieser, A.W., Gröbner, J., Blumthaler, M., Klotz, B., De Backer, H., Bolsée, D., Werner, R.,Tomsic, D., Metelka, L., Eriksen, P., Jepsen, N., Aun, M., Heikkilä, A., Duprat, T., Sandmann, H., Weiss, T., Bais, A., Toth, Z., Siani, A.M., Vaccaro, L., Diémoz, H., Grifoni, D., Zipoli, G., Lorenzetto, G., Petkov, B.H., Di Sarra, A.G., Massen, F., Yousif, C., Aculinin, A.A., Den Outer, P., Svendby, T., Dahlback, A., Johnsen, B., Biszczuk-Jakubowska, J., Krzyscin, J., Henriques, D., Chubarova, N., Kolarž, P., Mijatovic, Z., Groselj, D., Pribullova, A., Gonzales, J.R.M., Bilbao, J., Guerrero, J.M.V.,Serrano, A., Andersson, S., Vuilleumier, L., Webb, A., O'Hagan, J. UV Index monitoring in Europe (2017) Photochemical and Photobiological Sciences, 16 (9), 1349-1370

Siani, A.M., Modesti, S., Casale, G.R., Diemoz, H., Colosimo, A. Biologically effective surface UV climatology at Rome and Aosta, Italy (2013) AIP Conference Proceedings, 1531, 903-906, DOI: 10.1063/1.4804917

Siani, A.M., F. Frasca, F. Scarlatti, A. Religi, H. Diémoz, G. R. Casale, M. Pedone, V. Savastiouk Examination on total ozone column retrievals by Brewer spectrophotometry using different processing software, Atmos. Meas. Tech., 11, 5105–5123, 2018.

Slaper, H., Reinen, A. J. M., Blumthaler, M., Huber, M., and Kuik, F. Comparing ground-level spectrally resolved solar UV measurements using various instruments: a technique resolving effects of wavelength shift and slit width, Geophys. Res. Lett., 22, 2721–2724, 1995.

Vanicek, K. Differences between ground Dobson, Brewer and satellite TOMS-8, GOME-WFDOAS total ozone observations at Hradec Kralove, Czech. Atmos. Chem. Phys., 6, 5163–5171, 2006.

Takamura, T., and T. Nakajima, Overview of SKYNET and its activities, Opt. Pura Apl. 37, 3303-3308, 2004.